Some aspects of the mathematical modeling of prompt gamma neutron activation analysis

James Paul Holloway and Hatice Akkurt
University of Michigan
james.paul.holloway@umich.edu ; hatice.akkurt@umich.edu

ABSTRACT

We examine the mathematical structure of the non-linear problem determining the composition of a large, homogeneous, self-shielded material sample via prompt gamma neutron activation analysis. Composition determination is an inverse process, and requires a model which predicts the measured data as a function of composition. When the problem is written in terms of photopeak area ratios, as it should be to avoid absolute calibration issues, it is shown that this nonlinear problem always has a solution, independent of any of the details of the model. In the case of a large nearly pure sample it is shown that the composition of the trace elements can be determined uniquely, and that this composition is a continuous function of the measured peak area ratios. In the general case the issue of uniqueness and continuous dependence remain unclear, although these issues are related to the convergence properties of a fixed point iteration. We simulate this iteration with good effect for several materials. We also illustrate the issue of non-uniqueness with SiO_2, for which there is a non-unique relation between composition and the photopeak area ratio when certain gamma lines are used.

1. INTRODUCTION

Neutron activation analysis is a technique for determining the composition of materials, especially prized for its utility in finding the quantity of trace components in tiny samples. But it also can be used to quantify the major components of large samples, and in this respect it has been applied in areas such as coal assay, cement assay, and environmental studies.[1–6] But despite its worth as an analytical technique, there seems to have been little general, rigorous investigation of the modeling and mathematical issues of large sample activation analysis.

Classical activation analysis is greatly simplified by its use of small samples.[7] Such small samples can be activated in a neutron flux along with a multi-element reference material or a comparator, and subsequently gammas from these irradiated materials can be counted to determine the ratio of characteristic gammas from the sample to those from the reference; this ratio is taken to be directly proportional to the ratio of the number of diagnosed nuclei in the sample—which is desired—to that in the reference—which is known. This approach is self-calibrating: the source neutron flux need not be characterized, the detector efficiency is not needed, and even the activation cross sections cancel out. But this beauty is purchased at the price of analyzing only small samples in which neutron and gamma self-shielding can be ignored. Or it is purchased at the price of examining only trace elements in a sample of known bulk composition, and using a reference whose matrix is identical to that of the sample.

A much more complicated problem arises if activation analysis is attempted on large, bulk samples in which it is the bulk composition itself that is in question. Measurement techniques for large sample analysis are based on a combination of modeling and often extra measurements to correct or account for self-shielding effects. We will review some of these ideas below, but a key point is that the extra measurements required by such methods may not always be possible, and many methods tend to rely on the tractability of specific and approximate models such as one-speed diffusion theory. An important exception is a technique called Monte Carlo library least squares,[8] which is an *algorithm* for driving a transport model to a composition consistent with a measured gamma pulse height spectrum; the equations that we will analyze below are closely related to this.

In this paper we will examine the most basic large sample prompt gamma neutron activation analysis experiment, in which the bare minimum of measurements can be made on the sample, and in which models are asked to fill the information gap. We will ask if the problem of composition determination is a well posed problem in the mathematical sense. We will describe a general result, based on purely topological theorems, that rigorously addresses, but does not fully establish, the well posedness of the problem without reference to the details of the models.

2. MOTIVATION

The technique of prompt gamma neutron activation analysis is based on a measurement of the uncollided photons emitted by a sample that is being simultaneously exposed to neutrons. Those uncollided photons that deposit their full energy in the detector via a photoelectric interaction produce a signal which is characterized as a peak located at a well defined energy—the characteristic energy of the gamma being detected. The area under each such photopeak in the gamma spectrum is the fundamental measured quantity, but because absolute calibration of the source and detector is difficult, in practice the ratio of photopeak areas is the fundamentally useful quantity. The problem of neutron activation analysis is to use these photopeak area ratios, and perhaps other information about the sample, to determine the sample composition. This is fundamentally an inverse problem: there is a natural class of models that will, in principle, predict the photopeak areas generated by a

sample of given geometry, density and composition placed near a known neutron source, and the problem is to invert this model to determine composition from the measured photopeak area ratios.

The fundamental questions to consider when faced with this inverse problem are the questions of well-posedness:[9]

1. Given any (measured) set of photopeak area ratios, is there a composition to which they correspond? This is the question of existence.

2. Given any set of peak area ratios, is there more than one composition to which they correspond? This is the question of uniqueness.

3. Does the solution for composition, assuming it exists, tend to the true composition as errors in the measurement and model are reduced? This is a question of continuity of the composition as a function of photopeak areas, and a question of structural stability in the model.

Existence might easily be taken for granted—the sample certainly does have a composition! When we design the measurements, we do so with the expectation that we will gather enough information to fully determine composition; existence speaks to the confirmation, or not, of this expectation. Further, even if we have gathered the right information in the experiment, the determination of composition from a set of measurements requires the inversion of a *model*. We are not fully privy to nature's own truth, and there is no reason to believe that any model that we devise, based on imperfect understanding, approximations, and inexact physical data, will in fact be consistent with actual measurements.

The question of uniqueness might also be taken for granted—the sample certainly has only a single composition! But it is not obvious that there will be only a single composition that is consistent with a given set of measured peak areas. Since the measurement is not directly of composition, but rather is of photopeak area ratios that are only indirectly related to composition, why cannot two different compositions produce the same photopeak area ratios?

Finally, the issue of continuity and stability is practically important because we do not have a perfect model to invert, and because we do not have perfect measurements to base the inversion on. The errors of model and measurement will imply an error in the reconstructed composition, and it is important to know that as these errors are reduced the reconstructed composition will in fact become exact; this requires that the composition be a continuous function of the measured quantities and modeling parameters.

The most important result of this paper will deal with the question of existence. In part this speaks to the quantity of information needed: is a specific measurement setup sufficient, even in principle, to determine composition? Once we know that we have measured sufficient data, in principle, it might be argued that the existence of a solution for a specific model is of no practical consequence, since its absence is then simply the hallmark of a poor model. Surely all "sufficiently good" models will ensure the existence of a solution. This may not be true; it is possible that errors in

measurement will result in photopeak area ratios that are inconsistent with even a physically perfect model. But even if we set aside this concern, a confidence in the consistency between a sufficiently good model and the measurements does little to actually identify the features that mark a model as sufficiently good. The key result of this paper will be the identification of surprisingly weak, and physically essential, conditions on the model that ensure the existence of a sample composition that is consistent with measured photopeak area ratios.

3. PREVIOUS WORK

There is a large literature on the problem of composition determination via large sample prompt (and decay) gamma neutron activation analysis. Most of this work has been very focused on specific applications, and most of it therefore makes very specific assumptions about what can be measured and what physical behavior is important in the system. Often the goal is, at least implicitly, to formulate the problem of composition determination in a linear way, so that composition determination can be made directly from a set of measurements without any iteration. Unfortunately the exact physics speaks against this, so simplifying assumptions are always required in this kind of analysis, and the results are always approximate.

In order to provide information on the self-shielded neutron flux in the sample several authors have used computational transport codes.[2–4,6,10] This assumes an approximate composition in order to carry out the neutron transport, perhaps with extra measurements to support the determination of this approximate composition.[2] Others have used one speed diffusion theory solutions and used either extra measurements to determine the neutron diffusion coefficient and length,[11] or assumptions about the composition[12] appropriate for the specific application. In most of these models $1/v$ cross sections, Maxwellian thermal spectra, and sometimes separability of the flux, is assumed. In all of these approaches the goal is to determine sufficient information about the self-shielded neutron flux to allow an assessment of the gamma generation within the sample as a linear function of composition. Thus, the dependence of the neutron flux on composition is ignored.

There have also been a variety of approaches for determining the effects of gamma self-shielding. Wormald and Clayton[4] assume that the attenuation coefficient depends only weakly on energy, and actually ignore the energy dependence of the gamma attenuation coefficient in their model for coal analysis. Lapides et al.[2,3] used the existing photon cross section data but assumed a soil composition in their model for soil analysis, as did Savio et al.[12] in their concrete analysis. In contrast, Overwater et al.[13] measured the attenuation coefficients for selected gamma energies via a gamma transmission experiment through the sample. The goal of these approaches is again to avoid having any composition dependence in the gamma flux, and thus hide the nonlinearity of the problem.

The nonlinearity of the problem of composition determination via large sample activation analysis has certainly been noted before,[2,6,14,15] but little work has attacked it directly. This is not necessarily a mistake; the clever approach of Overwater et al., for example, effectively linearizes the

problem without any prior knowledge of the sample composition, although it does require solution of a nonlinear problem to determine one-speed diffusion theory parameters and it is dependent on assumptions that are not universally true.

One very significant exception to this linear focus is the so-called Monte Carlo library least squares method.[8,16] This method is an algorithm for solving the nonlinear problem of composition determination, driven by a neutron-photon transport code (the authors use Monte Carlo codes, hence the name, but in fact the use of Monte Carlo is not fundamental to the idea). The method was developed for full spectrum analysis in the days of NaI detectors, rather than for analysis based on well resolved individual photopeak areas, and is focused on a least squares fit to the measured spectrum of a linear combination of nuclide specific self-shielded pulse height spectra. The coefficients from this fit (presumably normalized, but this step is not explicitly mentioned) are taken to be the next iterate for composition of the sample. This composition is then used to generate new self-shielded spectra for the next round of spectrum fitting. The key point in the method then is that a transport model is used to compute a self-shielded neutron flux based on a previous composition iterate, and is used to compute the effect of gamma self-shielding, and these are then used to compute a new composition. The formulation of the problem that we analyze below is closely related to this algorithm.

4. MODEL OF THE BASIC PROBLEM

The most straightforward prompt gamma activation analysis setup, which will be the focus of our developments below, is as follows:

1. The bulk composition of a large sample of arbitrary size and of known density and geometry is to be determined. This sample is placed near a neutron source of known spectrum, and the neutrons interact in the sample to generate at least one detectable gamma line from each of the major nuclides in the sample. The gammas may interact in the sample, but some escape uncollided.

2. For a sample containing N major nuclides, N sufficiently strong gamma lines are detected in a nearby gamma spectrometer, one per nuclide, and all at distinct energies resolvable by the detector. These N photopeak areas, A_i, $i = 1 \ldots N$, are measured.

3. The sample composition, denoted by the weight fractions w_i, $i = 1 \ldots N$, for each of the N major nuclides is determined using only: the ratios of the photopeak areas, the sample density, the source–sample–detector geometry, the source spectrum, the relative efficiency of the detector, and microscopic cross-section data.

The reconstruction of composition is to be based only on the ratios of peak areas so that only relative measurements need be made, and a difficult absolute calibration of the neutron source or detector is unnecessary.

To set up the inverse problem our first task is to develop a class of models that will predict the peak areas A_i, $i = 1 \ldots N$, from the composition of the sample, specified as weight fractions w_i, $i = 1 \ldots N$. To simplify notation where appropriate, we will write $\mathbf{w}$ for a N-vector of the weight fractions w_i, $i = 1 \ldots N$, and $\mathbf{A}$ for a N-vector of the peak areas A_i, $i = 1 \ldots N$. Since we have one characteristic gamma per nuclide, we will, when useful, refer to a characteristic gamma energy E_i and the nuclide that creates it by the same index i.

Our primary hypothesis is that the photopeak area A_i in the i^{th} peak can be related to composition via models of the form

$$A_i = F_i(\mathbf{w}) w_i \tag{1}$$

where $F_i(\mathbf{w})$ is the peak area generated per weight fraction of nuclide i according to the model. We assume throughout that $F_i(\mathbf{w}) > 0$ and $F_i(\mathbf{w})$ is a continuous function of $\mathbf{w}$, for all $i = 1 \ldots N$.

Basic transport physics let's us flesh out a very complete model as

$$F_i(\mathbf{w}) = \int_\Delta d^2y \int_\Gamma d^3x \frac{S_i(\mathbf{x}, \mathbf{w}) e^{-\tau(E_i, \mathbf{x}, \mathbf{y}, \mathbf{w})}}{4\pi d^2(\mathbf{x}, \mathbf{y})} \frac{\hat{n} \cdot (\mathbf{y} - \mathbf{x})}{d(\mathbf{x}, \mathbf{y})} \epsilon(E_i, \mathbf{x}, \mathbf{y}) \tag{2}$$

where: $S_i(\mathbf{x}, \mathbf{w}) d^3x$ is the number, per weight percent nuclide i, of gammas of energy E_i emitted isotropically from the differential volume d^3x at $\mathbf{x}$, and its dependence on sample composition is shown explicitly; $d(\mathbf{x}, \mathbf{y})$ is the geometric distance from the point $\mathbf{x}$ in the sample Γ to the point $\mathbf{y}$ on the surface of the detector; $\tau(E_i, \mathbf{x}, \mathbf{y}, \mathbf{w})$ is the optical distance to gammas with energy E_i between those same two points, and this is again a function of composition; and $\epsilon(E_i, \mathbf{x}, \mathbf{y})$ is the probability that the detector will record a gamma traveling straight from $\mathbf{x}$ into the detector in the peak at E_i, given that the gamma has reached the detector surface at $\mathbf{y}$. The factor $d^2y\, \hat{n} \cdot (\mathbf{y} - \mathbf{x})/d(\mathbf{x}, \mathbf{y})$, with $\hat{n}$ the normal to the detector surface at $\mathbf{y}$, is the cosine of the angle between the normal and the direction of uncollided gamma travel, and hence when multiplied by the gamma fluence at $\mathbf{y}$ yields the number of gammas that enter the detector across d^2y at $\mathbf{y}$.

The gamma source $S_i(\mathbf{x}, \mathbf{w})$ can be written in terms of the (self-shielded) energy dependent neutron flux $\phi(\mathbf{x}, E, \mathbf{w})$ throughout the sample, and the gamma generation cross-section $\sigma_i(E)$, which is the neutron total cross section for nuclide i times the mean number of gammas of energy E_i that a neutron of energy E will generate when it interacts with nuclide i. In terms of these quantities we have

$$S_i(\mathbf{x}, \mathbf{w}) w_i = T \int_0^\infty \frac{N_0 \rho w_i \sigma_i}{M_i} \phi(\mathbf{x}, E, \mathbf{w}) dE\,, \tag{3}$$

where T is the counting time, N_0 is Avagadro's number, ρ is the known density of the sample, and M_i is the atomic weight of nuclide i. Except for this last, these quantities all scale out when we formulate the problem in terms of peak area ratios, although, except in some special infinite geometries, the sample density will still enter in determining the neutron flux and the optical pathlength in Eq. 2.

Note that in practice $F_i(\mathbf{w})$ will have to be determined approximately using some approximate neutron transport model, imperfectly known cross-section data, and approximate detector effi-

ciency model. Thus, the $F_i(\mathbf{w})$ used in the model will differ from the $F_i(\mathbf{w})$ that nature uses in the experiment.

Our view of the prompt gamma activation analysis problem is that, in principle, the measurement we have described should be enough. There are N weight fractions to be determined, and these must be normalized so that $1 = \sum_i^N w_i$, effectively meaning there are $N-1$ independent quantities to determine. There are N measured quantities A_i, $i = 1 \ldots N$, from which we will use only the $N-1$ independent ratios. The quantities that are needed to specify the functions $F_i(\mathbf{w})$, $i = 1 \ldots N$ can be determined based on neutron and photon transport models. So the setup seems sufficient; we prove below that it is.

5. HOMOGENEOUS FORMULATIONS AND EXISTENCE

As was described above, it is standard and sensible in practice to approach activation analysis problems using relative data, rather than absolute data, and thereby to eliminate difficult to determine quantities such as source strength and absolute detector efficiency. We must therefore write all of our expressions in a form that is homogeneous of degree zero in the photopeak areas.*

An obvious approach then is to take one of the equations, the N^{th} say, and divide all the others by it. The equations then become

$$\frac{A_i}{A_N} = \frac{F_i(\mathbf{w})w_i}{F_N(\mathbf{w})w_N} \qquad i = 1 \ldots N\,. \tag{4}$$

These $N-1$ equations (the N just says $1 = 1$), along with the normalization $1 = \sum_{i=1}^N w_i$, provide N equations for the N unknowns w_i. But this form is annoying, in that it singles out one nuclide in the denominator.

A more systematic, but equivalent, homogeneous formulation is useful. From Eq. 4 we can easily deduce that

$$\frac{A_i}{\sum_{j=1}^N A_j} = \frac{F_i(\mathbf{w})w_i}{F_N(\mathbf{w})w_N}\frac{A_N}{\sum_{j=1}^N A_j} \qquad i = 1 \ldots N \tag{5}$$

and so, summing Eq. 4 and eliminating the sum of the A_i on the right in Eq. 5, yields

$$\frac{A_i}{\sum_{j=1}^N A_j} = \frac{F_i(\mathbf{w})w_i}{\sum_{j=1}^N F_j(\mathbf{w})w_j} \qquad i = 1 \ldots N\,. \tag{6}$$

Thus, Eq. 4 implies Eq. 6, and in fact the reverse implication is straightforward to establish also.

*A function $\mathbf{w}(\mathbf{A})$ is homogeneous of degree zero if $\mathbf{w}(c\,\mathbf{A}) = \mathbf{w}(\mathbf{A})$ for any scalar c.

The form of Eq. 6 is homogeneous of degree zero in $\mathbf{A}$'s, and so solving it for $\mathbf{w}$ will result in solutions that do not depend on the absolute neutron source strength or absolute detector efficiency. Unfortunately, it is not immediately obvious under what conditions this system of equations has a solution, let alone one which satisfies the normalization $1 = \sum_{i=1}^{N} w_i$. We shall prove below that it does, by showing that the system of equations

$$w_i = \frac{A_i/F_i(\mathbf{w})}{\sum_{j=1}^{N} A_j/F_j(\mathbf{w})} \qquad i = 1 \ldots N \,. \tag{7}$$

does have solutions, and by showing that these equations capture all of the normalized solutions of Eq. 6. This equivalence is the subject of

LEMMA 1 *If* $\mathbf{A}$ *and* $\mathbf{w}$ *are related by Eq. 6 and* $1 = \sum_{i=1}^{N} w_i$*, then it is also true that* $\mathbf{A}$ *and* $\mathbf{w}$ *are related by Eq. 7. Conversely, if* $\mathbf{A}$ *and* $\mathbf{w}$ *are related by Eq. 7, then* $1 = \sum_{i=1}^{N} w_i$ *and* $\mathbf{A}$ *and* $\mathbf{w}$ *are also related by Eq. 6.*

Proof: Suppose first that $\mathbf{A}$ and $\mathbf{w}$ satisfy Eq. 6 with $1 = \sum_{i=1}^{N} w_i$. Then

$$w_i = \frac{A_i}{F_i(\mathbf{w})} \frac{\sum_{j=1}^{N} F_j(\mathbf{w}) w_j}{\sum_{j=1}^{N} A_j} \,, \tag{8}$$

and summing this must yield

$$1 = \sum_{i=1}^{N} (A_i/F_i(\mathbf{w})) \times \frac{\sum_{j=1}^{N} F_j(\mathbf{w}) w_j}{\sum_{j=1}^{N} A_j} \,, \tag{9}$$

or

$$\sum_{i=1}^{N} (A_i/F_i(\mathbf{w})) = \frac{\sum_{j=1}^{N} A_j}{\sum_{j=1}^{N} F_j(\mathbf{w}) w_j} \,. \tag{10}$$

Using this in Eq. 8 then yields

$$w_i = \frac{A_i/F_i(\mathbf{w})}{\sum_{i=1}^{N} A_i/F_i(\mathbf{w})} \tag{11}$$

which is Eq. 7.

To see the converse, note first by summing it that Eq. 7 implies that $1 = \sum_{i=1}^{n} w_i$, and that it also implies

$$F_i(\mathbf{w}) w_i = \frac{A_i}{\sum_{j=1}^{N} A_j/F_j(\mathbf{w})} \qquad i = 1 \ldots N \,. \tag{12}$$

This in turn yields

$$\sum_{j=1}^{N} F_j(\mathbf{w}) w_j = \frac{\sum_{j=1}^{N} A_j}{\sum_{j=1}^{N} A_j / F_j(\mathbf{w})} \,. \tag{13}$$

Dividing Eq. 12 by Eq. 13 yields

$$\frac{F_i \mathbf{w}_i}{\sum_{j=1}^{N} A_j / F_j(\mathbf{w})} = \frac{A_i}{\sum_{j=1}^{N} A_j} \qquad i = 1 \ldots N \,, \tag{14}$$

which is Eq. 6. Thus Eq. 7 implies Eq. 6.

■

We can now prove

THEOREM 1 *Suppose that $F_i(\mathbf{w}) > 0$ and is continuous for all i and all vectors $\mathbf{w}$ with non-negative components. Let any $\mathbf{A} \neq 0$ and with non-negative components be given. Then there is at least one $\mathbf{w}$ with non-negative components that satisfies Eq. 6 with $1 = \sum_{i=1}^{N} w_i$; the same $\mathbf{A}$ and $\mathbf{w}$ satisfy Eq. 7. This solution is homogeneous of degree zero in $\mathbf{A}$, and $w_i = 0$ if and only if $A_i = 0$.*

Proof: By Lemma 1 we need prove the theorem only for Eq. 7, since the normalized solutions of Eq. 6 and 7 are the same.

First, the trivial bits. The condition $F_i(\mathbf{w}) > 0$ ensures that the right-hand-side in Eq. 7 is well defined, and ensures that it is non-negative for all $i = 1 \ldots N$ when the components of $\mathbf{A}$ are non-negative, as assumed. Note that if $\mathbf{w}$ satisfies Eq. 7 then, as seen simply by summing the equation over i, it must be that $1 = \sum_{i=1}^{N} w_i$. Further, if $A_i = 0$ for some i, then Eq. 7 implies that $w_i = 0$ for the same i. Conversely, if $w_i = 0$ for some solution of Eq. 7, then, again directly from Eq. 7, $A_i = 0$ also. That the solution is homogeneous of degree zero in $\mathbf{A}$ follows from the invariance of the right-hand-side of Eq. 7 under the substitution $\mathbf{A} \to c\,\mathbf{A}$.

To prove existence, now let $\mathcal{P}$ denote the set of physically realizable composition vectors, $\mathcal{P} = \{\mathbf{w} \in \mathbf{R}^N | 1 = \sum_{i=1}^{N} w_i, w_i \geq 0, i = 1 \ldots N\}$; note that $\mathcal{P}$ is a closed and bounded, convex set. Now, for a given $\mathbf{A}$ define the continuous nonlinear vector valued mapping $\mathbf{G} : \mathbf{R}^N \to \mathbf{R}^N$ by it's components

$$G_i(\mathbf{w}) = \frac{A_i / F_i(\mathbf{w})}{\sum_{j=1}^{N} A_j / F_j(\mathbf{w})} \,. \tag{15}$$

Note that for $\mathbf{A}$ with non-negative components, $\mathbf{G}$ maps $\mathcal{P}$ into itself. Therefore, by the Brouwer fixed point theorem (which, for completeness, is described in the appendix), $\mathbf{G}$ has a fixed point in $\mathcal{P}$, i.e. there is a $\mathbf{w} \in \mathcal{P}$ such that $\mathbf{w} = G(\mathbf{w})$. From the definition of $\mathbf{G}$, this fixed point of $\mathbf{G}$ is a solution of Eq. 7

■

This theorem says that in an N component system, a composition can be found that makes *any* transport model consistent with *any* set of $N-1$ measured peak area ratios. This is true as long as the transport model guarantees a positive peak area per weight fraction for each nuclide, which is an essentially trivial requirement, as an examination of Eqs. 2 and 3 reveals.

General results on the continuity and uniqueness of the solution $\mathbf{w}$ as a function of the peak areas $\mathbf{A}$ are not in hand. The two are related, of course; if the functions F_i are smooth then the implicit function theorem[17] states that the solution as a function of $\mathbf{A}$ is continuous except at bifurcation points, that is, except at points of local non-uniqueness. However, actually exploiting the implicit function theorem to develop concrete results is difficult, because such results will depend on the derivatives of $F_i(\mathbf{w})$, and these will in turn depend on the complicated details of the transport physics. We do have a result in one special case: in a sample consisting of a sufficiently pure matrix $\mathbf{w}(\mathbf{A})$ will be unique and depend continuously on $\mathbf{A}$. This is the content of

THEOREM 2 *Let $\bar{\mathbf{A}}$ denote the vector with $\bar{A}_1 = 1$ and $\bar{A}_j = 0$, $j \neq 1$, and suppose that $F_i(\mathbf{w})$ is a smooth function otherwise satisfying the conditions of Theorem 1. Then there is a neighborhood of $\bar{\mathbf{A}}$ in which the solution $\mathbf{w}(\mathbf{A})$ of Eq. 7 (or equivalently the normalized solutions of Eq. 6) is unique and a continuous function of $\mathbf{A}$.*

Proof: Consider the function $\mathbf{G}$ defined in the proof of Theorem 1; this function is smooth in both $\mathbf{w}$ and $\mathbf{A}$ (in a neighborhood of $\bar{\mathbf{A}}$) because the functions $F_i(\mathbf{w})$, $i = 1 \ldots N$ are smooth. For a given $\mathbf{A}$, a vector $\mathbf{w}$ satisfies Eq. 7 if and only if $0 = \mathbf{w} - G(\mathbf{w}, \mathbf{A})$, where we have emphasized the smooth $\mathbf{A}$ dependence of $\mathbf{G}$ as well. Note also that the pair $\bar{\mathbf{w}}, \bar{\mathbf{A}}$, with $\bar{w}_1 = 1$ and $\bar{w}_j = 0$, $j \neq 1$, satisfy $0 = \bar{\mathbf{w}} + G(\bar{\mathbf{w}}, \bar{\mathbf{A}})$. We can therefore use the implicit function theorem to explore the dependence of the solution $\mathbf{w}(\mathbf{A})$ on $\mathbf{A}$ in a neighborhood of $\bar{\mathbf{A}}$.

Let $H(\mathbf{w}, \mathbf{A}) = \mathbf{w} - G(\mathbf{w}, \mathbf{A})$. Then $H(\bar{\mathbf{w}}, \bar{\mathbf{A}}) = 0$, and the Jacobian matrix of H with respect to $\mathbf{w}$ at this point, denoted $D_{\mathbf{w}}H(\bar{\mathbf{w}}, \bar{\mathbf{A}}) = I + D_{\mathbf{w}}G(\bar{\mathbf{w}}, \bar{\mathbf{A}})$, where I is the identity matrix. The implicit function theorem tells us that if $D_{\mathbf{w}}H(\bar{\mathbf{w}}, \bar{\mathbf{A}})$ is invertible, then $H(\mathbf{w}, \mathbf{A}) = 0$ will have a unique solution for $\mathbf{w}$ near $\mathbf{A} = \bar{\mathbf{A}}$ and $\mathbf{w} = \bar{\mathbf{w}}$, and this solution $\mathbf{w}(\mathbf{A})$ will be a smooth function of $\mathbf{A}$. Since $D_{\mathbf{w}}H(\bar{\mathbf{w}}, \bar{\mathbf{A}})$ is a perturbation of the identity, it is invertible if $\|D_{\mathbf{w}}G(\bar{\mathbf{w}}, \bar{\mathbf{A}})\| < 1$.

For the case at hand we can compute the elements of G at $\mathbf{A} = \bar{\mathbf{A}}$ as $G_1(\mathbf{w}, \bar{\mathbf{A}}) = 1$ and $G_j(\mathbf{w}, \bar{\mathbf{A}}) = 0$, $j \neq 1$. Therefore the Jacobian $D_{\mathbf{w}}G(\bar{\mathbf{w}}, \bar{\mathbf{A}}) = 0$, and so $D_{\mathbf{w}}H(\bar{\mathbf{w}}, \bar{\mathbf{A}})$ is invertible, and this proves the theorem.

■

This result is not as useful as we would wish, as it only addresses the case of small perturbations to a nearly pure sample. However, it does connect our analysis to the case of large sample activation analysis of trace composition in a nearly pure matrix. In this case the nonlinearity of the problem will not introduce any local non-uniqueness or discontinuities.

6. A FIXED POINT ITERATION

The form of Eq. 7 as a fixed point problem immediately suggests an iteration for its solution, namely

$$w_i^{n+1} = \frac{A_i/F_i(\mathbf{w}^n)}{\sum_{j=1}^N A_j/F_j(\mathbf{w}^n)} \qquad i = 1 \ldots N \tag{16}$$

where n is the iteration number; in vector notation we write this iteration as $\mathbf{w}^{n+1} = \mathbf{G}(\mathbf{w}^n)$. This iteration is essentially the iteration carried out in the Monte Carlo library least squares method,[18] whose convergence has been observed to be fast, but has never been rigorously studied. In this section we will describe some observations on the iteration of Eq. 16.

There are a number of theorems on the convergence of fixed point iterations, the simplest and most powerful being Banach's fixed point theorem.[17] Unfortunately, useful application of these theorems will require exploiting the details of the radiation transport model. There is a connection between convergence of the fixed point iteration, uniqueness, and continuity that Banach's fixed point theorem provides: if the Jacobian matrix $D_{\mathbf{w}}\mathbf{G}$ of the function $\mathbf{G}$ is bounded as $\|D_{\mathbf{w}}\mathbf{G}\| < 1$ uniformly in $\mathbf{w}$ for a fixed $\mathbf{A}$, then the mapping $\mathbf{G}$ is a contraction mapping and the fixed point iteration of Eq. 16 will converge quickly independent of the initial guess $\mathbf{w}^0$, there will be only one solution of Eq 7, and that solution will be a continuous function of $\mathbf{A}$. However, to date we have not been able to develop useful conditions to ensure the uniform bound $\|D_{\mathbf{w}}\mathbf{G}\| < 1$ for anything other than toy models, and even in those toy models the conditions have proven to depend on details of cross sections which are sometimes true, and sometimes not, for real cross sections. This does open the possibility that the iteration might sometimes fail to converge, and it opens the possibility that there could be a non-uniqueness of the solution of the problem for composition. We will support this assertion below.

To illustrate some of these issues, we have carried out the fixed point iteration for realistic systems using a neutron-photon Monte Carlo code, MCNP.[19] Because we do not yet have experimental measurements to explore, we begin these simulations by computing the photopeak areas $\mathbf{A}^*$ from a sample of specified composition $\mathbf{w}^*$; these values $\mathbf{A}^*$ are then the "measured" peak areas, and $\mathbf{w}^*$ is the "unknown" composition.* Then, for any arbitrary composition $\mathbf{w}$ we can compute the values of the functions $F_i(\mathbf{w})$ by using the Monte Carlo code to compute the number of gammas, $\mathbf{A}(\mathbf{w})$, emitted by the sample and detected in a detector, from which we then define the function value $F_i(\mathbf{w}) = a_i(\mathbf{w})/w_i$. This allows us to run the iteration

$$w_i^{n+1} = \frac{A_i^*/F_i(\mathbf{w}^n)}{\sum_{j=1}^N A_j^*/F_j(\mathbf{w}^n)} \qquad i = 1 \ldots N \tag{17}$$

and see if $\mathbf{w}^n \to \mathbf{w}^*$, and what impact the initial guess $\mathbf{w}^0$ may have.

*In some tests we have added errors to $\mathbf{A}^*$ to simulate measurement errors, and to make the peak areas inconsistent with the exact composition $\mathbf{w}^*$. The results of these tests are unsurprising, and are not described in the results reported here.

We have carried out these simulations for two different geometries: one consists of a 14MeV neutron point source placed on the surface of a semi-infinite slab sample, with all escaping gammas detected; the other contains a 14MeV neutron point source at the center of a spherical sample, with all gammas that escape the outer surface of the sphere detected. A 14 MeV neutron source is used because it's neutrons are high enough to allow inelastic scatter off of the second excited state of O-16; this is the most useful means to produce a detectable gamma signal from O-16 (the first excited state is a 0^+ state, and will therefore not decay by gamma emission to the 0^+ ground state).

The simulations reported here were performed using the coupled neutron-photon transport mode of MCNP-4B (we have also undertaken similar iterations with TART98,[20] but this code provides well resolved gamma lines only for inelastic scatter gammas). The photons that reach the detector without suffering any collision were recorded using the particle trac option of the code. The energies of the emitted photons were then extracted from the trac file, and the number of uncollided photons reaching the large detector zone and having the correct characteristic energy for a particular nuclide were sorted and summed using a separate code. This approach obviously has advantages compared to attempting to simulate the pulse height spectrum from the gamma flux calculations[21] or calculating the photopeak area by numerically integrating Eq. 2 using the computed neutron flux spectrum[22], and produces smaller variances than using point detectors to estimate the uncollided photopeak areas.[14,15] The drawback of this approach is the size of the particle trac file, which unfortunately is very large.

MCNP has been used before for simulating prompt gamma analysis,[15,23] especially for well-logging[21] applications. As part of a well-logging project, the quality of the photon production cross sections were reviewed.[24] It was concluded that the photon production cross sections from the ENDF/B-V and ENDF/B-VI libraries are equivalent for most of the nuclides, but that the ENDF/B-VI library is moderately better for some nuclides (e.g. Mn). However, the ENDF/B-V library includes some gamma lines that were lost when the ENDF/B-VI based libraries were generated. Further, the data for Mg and Fe have large equal probability bins producing no resolved gamma lines. For Fe the T2 evaluation is better because of its finer energy resolution compared to ENDF/B-V and ENDF/B-VI libraries, and it was used in the simulations performed here. But for Mg the bin width is a large 250 keV and there are no well resolved gamma lines available in the libraries distributed with MCNP*. Because of this problem with Mg data, the SRM-668 simulation described below was performed by excluding Mg from the composition. The bin width for calcium capture gamma lines is 10 keV whereas the resolution is much better for the 1.158 MeV inelastic scatter line.[25] In general then, the quality of the photon production data is not adequate for experimental use in this kind of application. But it will serve for the illustrations presented here.

To first illustrate the observed rapid convergence of the iteration, Fig. 1 shows the convergence history of a ternary system made up of a 10 cm sphere of iron, chromium and nickel, in a composition representative of 316 stainless steel; the initial guess is equal weights of Fe-Cr-Ni. Carbon and trace elements are not included in this system, although we have also applied the method to an Fe-C system with similar convergence results. We see from the figure that only a few iterations are

*TART also uses the ENDF/B-VI photon production data, but it has a strong gamma line for Mg at 1.369 MeV. This might suggest that this gamma line was lost while processing the data for MCNP

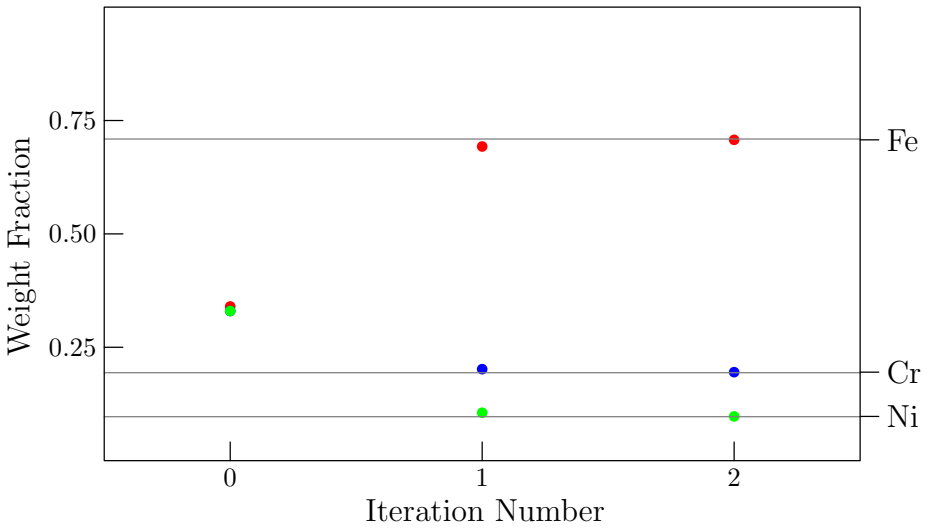

Figure 1: Convergence of the fixed point iteration to the composition of a stainless steel. Red points are Fe fraction, blue are Cr, and green are Ni; the grey lines represent the correct composition of the sample.

required to converge the composition.

For an illustration involving a much more complex system, Fig. 2 shows the convergence history of the iteration applied a basaltic rock based on the well characterized NBS standard reference material SRM-688 basalt. The geometry in this case is a half-infinite slab with a 14 MeV point neutron source placed on its surface, and with all emitted gammas detected. The sample composition includes several trace elements not shown in the figure; these trace elements do not prevent convergence to the composition of the major constituents, and their composition is also determined by the iteration, but with less relative accuracy due to the small number of gammas emitted by these trace elements. In both the stainless steel and the basaltic rock, the fixed point iteration has been observed to converge rapidly to the true sample composition independent of initial guess. This is characteristic of a contraction mapping.

However, the very much simpler silica, SiO_2, provides somewhat more insight into the issue of non-uniqueness. Figure 3 shows the fixed point iteration applied to a half-infinite slab of silica starting from a wildly wrong initial composition guess of 90% Si; the gamma lines used in this iteration are the 1779 keV inelastic scatter gamma from the first excited state of Si-28 and the 6129 keV inelastic scatter gamma from the second excited state of O-16. Only a few iterations are required to recover the correct composition, and other runs tell us that this fixed point is achieved independent of the initial guess. Again the behavior is characteristic of a contraction mapping.

In this binary system this behavior can be understood by noting that the normalized solutions for composition satisfy $w_{\mathrm{Si}} = G_{\mathrm{Si}}(w_{\mathrm{Si}}, w_{\mathrm{O}}, \mathbf{A}^*)$, with $w_{\mathrm{O}} = 1 - w_{\mathrm{Si}}$. Thus $w_{\mathrm{Si}} = G_{\mathrm{Si}}(w_{\mathrm{Si}}, 1 - w_{\mathrm{Si}}, \mathbf{A}^*)$, which is a one-dimensional fixed point problem for the silicon weight fraction. The function G_{Si} with $\mathbf{A}^*$ from SiO_2 from the 1779 keV Si and 6129 keV O gammas, as a function of silicon weight

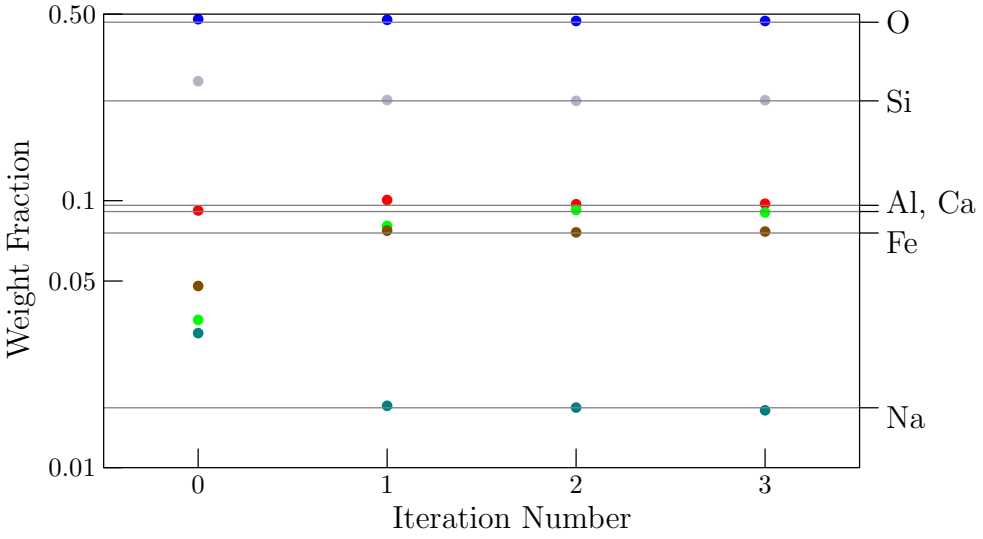

Figure 2: Convergence of the fixed point iteration to the composition of a basaltic rock (NBS Standard Reference Material SRM-688). The weight fraction scale is logarithmic. The grey lines again indicate the correct weight fractions for each element, as marked on the right.

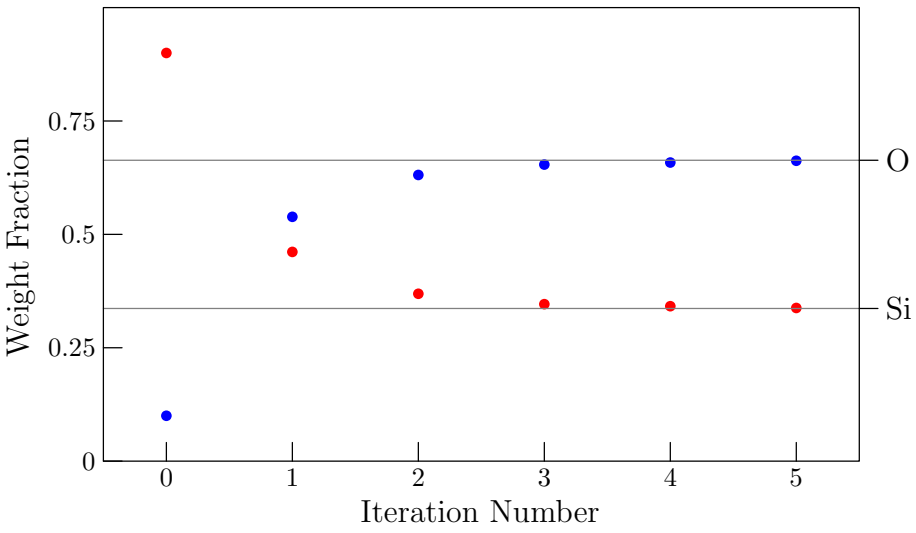

Figure 3: Convergence history of the fixed point iteration to the composition of SiO_2. The grey lines mark the correct composition.

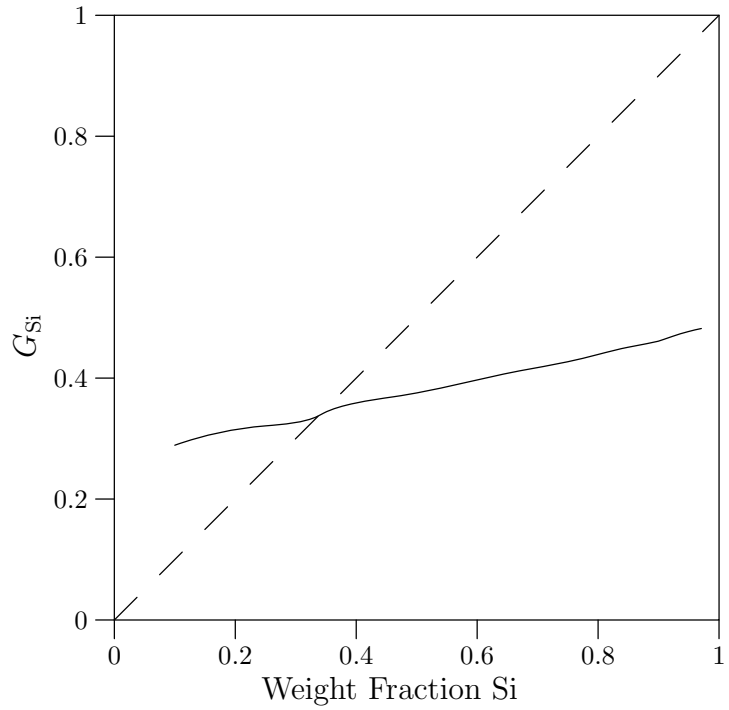

Figure 4: The function G_{Si} as a function of Si weight fraction, for the 1779 keV Si and 6129 O gammas from silica. The intersection with the diagonal line is the fixed point, which is the composition of silica.

fraction, is shown in Fig. 4. The slope of this function is pretty clearly less than 1 everywhere, implying that $\mathbf{G}$ is a contraction mapping and so that there is a unique solution of the fixed point problem, and this fixed point composition can be found using the fixed point iteration of Eq. 16.

However, if we use the 3539 keV radiative capture gamma from Si along with the 6129 keV inelastic scatter gamma from O to define $\mathbf{A}^*$, very different behavior occurs. Fig. 5 shows the function G_{Si} as a function of weight fraction Si for these gammas using the expected SiO_2 photopeak areas. In this case there are three fixed points of G_{Si}. Two can be seen in the intersection with the diagonal line; a third will exist near $w_{\mathrm{Si}} = 1$ because $G_{\mathrm{Si}} \leq 1$ by definition, but we have not attempted to explicitly compute it. Because of the equivalence between Eq. 7 and the normalized solutions of Eq. 6 each of these three fixed points represents a mixture of Si and O for which the photopeak area ratio of 3539 keV Si-gammas to 6129 keV O-gammas is equal to the area ratio for SiO_2. This means that the fixed point iteration cannot converge independent of initial guess, and it suggests that bifurcations could occur, leading to discontinuous relations between photopeak area ratios and composition. The iteration will converge if the initial guess is near the correct composition, but an initial guess that is not sufficiently good will lead to convergence to the fixed point near $\mathbf{w}_{\mathrm{Si}} = 1$.

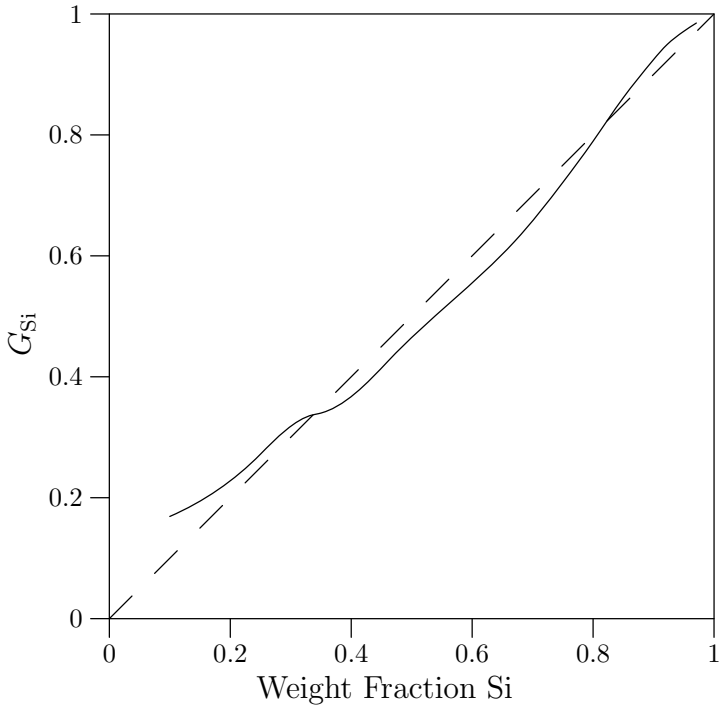

Figure 5: The function G_{Si} for SiO_2 as a function of Si weight fraction, for the 3539 keV Si and 6129 O gammas from silica. There are now three fixed points of G_{Si}, that is, three different mixtures of Si and O that yield the same photopeak area ratio as SiO_2. (Only two of the fixed points can be explicitly seen; the third is near $w_{\mathrm{Si}} = 1$)

7. CONCLUSIONS

In general, the relation between sample composition and detected gamma photopeak area ratio is nonlinear, and this nonlinearity makes the problem of composition determination difficult to analyze. In this paper we have applied some tools from nonlinear functional analysis in order to develop some rigorous results on the nature of this problem. In particular, we have established that any reasonable neutron and photon transport model—even a highly inaccurate one—is consistent with any measured gamma peak area ratios—even highly inaccurate ones. In general the issues of uniqueness and continuity remain somewhat open. The case of determining trace composition in a nearly pure matrix can be fully analyzed, and is well posed.

We have developed these results using a formulation of the large sample prompt gamma activation analysis problem that is homogeneous of degree zero in the measured gamma peak areas, and which always has a solution. We have also shown that this homogeneous formulation is equivalent to a fixed point problem. The fixed point iteration is especially useful in practice because it does not require any derivatives of the nonlinear function, as would, for example, Newton's method. While we have not proven any useful convergence results for this iteration, we have applied it in simulation, with good effect, and it is effectively equivalent to the Monte Carlo library least squares method.

Quite realistic computational examples suggest that there could be multiple solutions for the composition as a function of gamma peak area ratios. Such multiple solutions have negative implications for the convergence of the fixed point iteration, and for the continuity of the composition as a function of area ratios and modeling parameters. Understanding general conditions that preclude the appearance of such multiple solutions is an open area of inquiry.

Acknowledgements

The authors would like to acknowledge many useful discussions with Ronald F. Fleming of the University of Michigan. The second author (HA) has been supported in this work by the Horace H. Rackham School of Graduate Studies.

Brouwer Fixed Point Theorem

THEOREM 3 *(Brouwer) Let* $\mathbf{G}$ *be a continuous map from a closed, bounded, convex subset of* $\mathbf{R}^N$ *to itself. Then there is a fixed point* $\mathbf{w}$*,* $\mathbf{w} = \mathbf{G}(\mathbf{w})$*, of the map in that set.*

Many proofs exist of this amazing theorem;[17] most modern proofs are based on topological degree theory. In one-dimension the theorem is trivial, while in higher dimensions it is rather difficult to prove.

References

[1] Larry G. Evans, Jacob I. Trombka, Jeffrey R. Lapides, and Dal H. Jensen. Determination of elemental composition in geochemical exploration using a 14-MeV neutron generator. I. experimental aspects. *IEEE Transactions on Nuclear Science*, NS-28:1626–1628, 1981.

[2] Jeffrey R. Lapides, Larry G. Evans, and Jacob I. Trombka. Determination of elemental composition in geochemical exploration using a 14-MeV neutron generator. II. theoretical aspects. *IEEE Transactions on Nuclear Science*, NS-28:1629–1631, 1981.

[3] Larry G. Evans, Jeffrey R. Lapides, Jacob I. Trombka, and Dal H. Jensen. In situ elemental analysis using neutron-capture gamma-ray spectroscopy. *Nuclear Instruments and Methods*, 193:353–357, 1982.

[4] M. R. Wormwald and C. G. Clayton. In situ analysis of coal by measurement of neutron-induced prompt γ-rays. *International Journal on Appliations of Radiation and Isotopes*, 34:83–93, 1983.

[5] Keisuke Sueki, Kanako Kobayashi, Wataru Sato, Hiromichi Nakahara, and Takeshi Tomizawa. Nondestructive determination of major elements in a large sample by prompt γ ray neutron activation analysis. *Analytical Chemistry*, 68:2203–2209, 1996.

[6] Stephen L. Howell, Raymond A. Sigg, Frank S. Moore, and Timothy A. DeVol. Nondestructive bulk soil analysis for a chlorinated compound using prompt gamma-ray neutron activation analysis. In *Proceedings of the Tenth International Conference on Modern Trends in Activation Analysis*, April 1999.

[7] Zeev B. Alfassi. Principles of activation analysis. In Zeev B. Alfassi, editor, *Activation Analysis*, volume I. CRC Press, 1990.

[8] C. M. Shyu, R. P. Gardner, and K. Verghese. Development of the Monte Carlo library least-squares method of analysis for neutron capture prompt gamma-ray analyzers. *Nuclear Geophysics*, 7:241–267, 1993.

[9] V. B. Glasko. *Inverse Problems of Mathematical Physics*. American Institute of Physics, 1988.

[10] S. L. Shue, R. E. Faw, and J. K. Shultis. Thermal-neutron intensities in soils irradiated by fast neutrons from point sources. *Chemical Geology*, 144:47–61, 1998.

[11] Ronald W. Overwater and J. E. Hoogenboom. Accounting for the thermal neutron flux depression in voluminous samples for instrumental neutron activation analysis. *Nuclear Science and Engineering*, 117:141–157, 1994.

[12] D. L. C. Savio, M. A. J. Mariscotti, and S. R. Guevara. Elemental analysis of a concrete sample by capture gamma rays with a radioisotope neutron source. *Nuclear Instruments and Metods in Physics Research*, B95:379–388, 1995.

[13] Ronald W. Overwater, Peter Bode, and Jeroen J. M. de Goeij. Gamma-ray spectroscopy of voluminous sources: corrections for source geometry and self-attenuation. *Nuclear Instruments and Methods in Physics Research*, A324:209–218, 1993.

[14] C. Oliveira, J. Salgado, I. F. Goncalves, F. G. Carvalho, and F. Leitao. A monte carlo study of the influence of the geometry arrangements and structural materials on pgnaa system performance for cement raw materials. *Applied Radiation and Isotopes*, 48:1349–1354, 1997.

[15] C. Oliveira, J. Salgado, and F. G. Carvalho. Optimization of pgnaa instrument design for cement raw materials using mcnp code. *Journal of Radioanalytical and Nuclear Chemistry*, 216:191–198, 1997.

[16] K. V. Verghese and R. P. Gardner. A generalized approach to designing specific-purpose monte carlo programs: a powerful simulation tool for radiation applications. *Nuclear Instruments and Methods in Physics Research*, A299:1–9, 1990.

[17] Klaus Deimling. *Nonlinear Functional Analysis*. Springer-Verlag, 1985.

[18] T. He, R. P. Gardner, and K. Verghese. The Monte Carlo library least-squares approach for energy dispersive x-ray fluorescense analysis. *Applications of Radiation and Isotopes*, 44:1381–1388, 1993.

[19] Judith F. Briesmeister. MCNP–a general n-particle transport code. Technical Report LA-12625-M, Los Alamos National Laboratory, 1997.

[20] Dermott E. Cullen. TART98: A coupled neutron-photon 3d combinatorial geometry time dependent monte carlo transport code. Technical Report UCRL-ID-126455, Lawrence Livermore National Laboratory, 1998.

[21] Richard C. Odom, Shawn M. Bailey, and Robert D. Wilson. Benchmarking computer simulations of neutron-induced, gamma-ray spectroscopy for well logging. *Applied Radiation and Isotopes*, 48:1321–1328, 1997.

[22] S. L. Shue, R. E. Faw, and J. K. Shultis. Thermal-neutron intensities in soild irradiated by fast neutrons from point sources. *Chemical Geology*, 144:47–61, 1998.

[23] R. P. Gardner, A. Sood, Y. Y. Wang, L. Liu, P. Guo, and R. J. Gewhrke. Single peak versus library least-squares analysis methods for the pgnaa analysis of vitrified waste. *Applied Radiation and Isotopes*, 48:1331–1335, 1997.

[24] Stephanie C. Frankle. Photon production assessment for the MCNP data libraries. Technical Report LA-13092-MS, Los Alamos National Laboratory, 1996.

[25] J. Comly. Discrete-energy gamma-rays from mcnp data libraries. Technical Report LA-UR-98-535, Los Alamos National Laboratory, 1997.